nature reviews genetics

https://doi.org/10.1038/s41576-025-00869-4

Review article

Check for updates

Towards improved fine-mapping of candidate causal variants

Zheng Li [1,2] & Xiang Zhou [1,2]

Abstract

Fine-mapping in genome-wide association studies aims to identify potentially causal genetic variants among a set of candidate variants that are often highly correlated with each other owing to linkage disequilibrium. A variety of statistical approaches are used in fine-mapping, almost all of which are based on a multiple regression framework to model the relationship between genotype and phenotype, while accommodating specific assumptions about the distribution of variant effect sizes and using different inference algorithms. Owing to their modelling flexibility and the ease of making inferential statements, these approaches are predominantly Bayesian in nature. Recently, these approaches have been improved by refining modelling assumptions, integrating additional information, accommodating summary statistics, and developing scalable computational algorithms that improve computation efficiency and fine-mapping resolution.

Sections

[1]Department of Biostatistics, University of Michigan, Ann Arbor, MI, USA. [2]Center for Statistical Genetics, University of Michigan, Ann Arbor, MI, USA. e-mail: xzhousph@umich.edu

Introduction

Genome-wide association studies (GWAS) have identified thousands of genetic variants, primarily single-nucleotide polymorphisms (SNPs), associated with various diseases or disease-related complex traits[1–4]. However, many of these associations are likely not causal owing to linkage disequilibrium (LD), in which non-causal variants are nonrandomly associated with causal variants within local genomic regions[2,5]. To distinguish causal variants from a potentially large set of non-causal variants, fine-mapping studies, typically beginning with statistical fine-mapping analysis, are often conducted[6–10] (Box 1). These studies have refined sets of potentially causal variants, have enabled analysis across multiple ancestries[11,12] and traits[13,14], have improved the transferability of polygenic scores across ancestries[15], and have provided key insights into the genetic architecture[11–14] and biological mechanisms underlying diseases and complex traits[16].

One of the earliest and simplest strategies for fine-mapping involves selecting the top genetic variants with the strongest GWAS association evidence in the local region. However, owing to high LD, stochastic variability and the possible presence of multiple causal variants, the top associations in a local region are often non-causal, rendering this simple strategy ineffective[17–19] (Fig. 1a). Instead, it is preferable to jointly model all SNPs in the local region, as has been done in other fine-mapping contexts in which each SNP is tested for an association conditional on all other SNPs[20], but this approach is ineffective owing to the large number of SNPs. Alternatively, a commonly applied stepwise conditional analysis approach utilizes a 'greedy' search algorithm that first selects the top variant and then iteratively tests for additional variants, while adjusting for those already included in the model, until no further variant reaches a pre-specified significance threshold[21]. (Notably, such conditional analyses are also commonly used to identify secondary association signals[22,23].) However, conditional analyses cannot assess the statistical uncertainty of the identified variants because the strategy is greedy in nature and does not consider other possible combinations of variants that could explain the association equally well, or even better. For example, when two variants are in perfect LD and only one is causal, the order in which they are evaluated in the conditional analysis would result in the first variant being included and the second variant being excluded, leading to a 50% chance of not identifying the causal variant[17,19] (Fig. 1b). To account for such cases, other fine-mapping strategies have been developed to identify groups of highly correlated variants and provide probabilistic measures of uncertainty for both the presence of causal variants within each group and the likelihood of each variant being causal[19].

The fine-mapping methods that identify groups of variants and ascribe probabilities of causality are predominately based on a Bayesian framework, owing to its modelling flexibility and straightforwardness in making the necessary inferential statement[19,24–27] (Fig. 1c). Such Bayesian methods have benefited from recent improvements in power and resolution by increasingly integrating data from multiple sources, including variant functional annotations[28,29], multiple genetic ancestries[11,12] and correlated traits[14]. Additionally, many of these methods are now designed to work with GWAS summary statistics to maximize applicability while addressing privacy constraints[30].

In this Review, we discuss recent advances in statistical fine-mapping, with an emphasis on methods based on a Bayesian framework (Table 1; other frameworks have been reviewed elsewhere[7,31,32]). We begin with a description of the general fine-mapping workflow and basic statistical outputs, followed by an overview of the statistical modelling framework and how different methods can be understood within such framework as making distinct modelling assumptions about variant effect sizes and using different algorithms for inference. Next, we discuss recent work to improve fine-mapping methods by integrating additional information, such as functional annotations, multiple traits, multiple genetic ancestries and gene expression studies. Finally, we conclude by highlighting the key analytical challenges that remain unsolved.

Box 1 | Statistical versus biological causality

Statistical fine-mapping aims to identify a minimal set of potential causal variants using statistical methods to inform functional experimental studies[6,10,132,133]. The variants identified through statistical fine-mapping are considered causal in a statistical sense — that is, they are likely to explain the observed association signals given the data and model assumptions. Although the associations between statistically fine-mapped variants and the trait are unlikely to result from reverse causation, they may still be influenced by confounding factors that are not fully controlled owing to inevitable model misspecification. This notion of statistical causality differs from biological causality, which implies a direct mechanistic role in trait or disease aetiology and requires validation through experimental studies. Statistical fine-mapping methods typically produce credible sets with pre-specified confidence levels, offering a principled approach to uncertainty quantification that balances statistical power with control of false discoveries.

General workflow and basic statistical outputs

Data pre-processing and quality control

A typical fine-mapping workflow (Fig. 2) begins with either individual-level genotype and phenotype data or GWAS summary statistics as input. The analytic process starts by defining genomic loci within a specific distance, typically 1 MB, from genetic variants significantly associated with the phenotype of interest. Overlapping loci are then merged into a final set of loci ready for analysis. For individual-level data, the workflow conducts standard quality control on samples and variant genotypes[2]. Additionally, the phenotype of interest is typically processed by adjusting for confounding factors (for example, age, gender and population stratification) through regression, resulting in phenotype residuals that are used in subsequent fine-mapping analyses. For GWAS summary statistics, the workflow also includes quality control steps, such as excluding SNPs with a low minor allele frequency (MAF), strand ambiguity or potential mismatches between *z*-scores (that is, a list of marginal association measures between SNPs and the phenotype) and the LD matrix (that is, a table of pairwise correlations between SNPs). To address these potential mismatches, analytic tools have been developed to detect and remove outlier SNPs whose summary statistics may not match the LD reference owing to inter-cohort heterogeneity or mismatched reference data (but challenges remain, as discussed later)[30,33,34]. Additionally, regularization of the LD matrix can be applied to improve the consistency between *z*-scores and the LD matrix[30], and, when necessary, reference and alternative alleles are flipped so that the data used to compute *z*-scores and the LD matrix correspond to the same set of alleles.

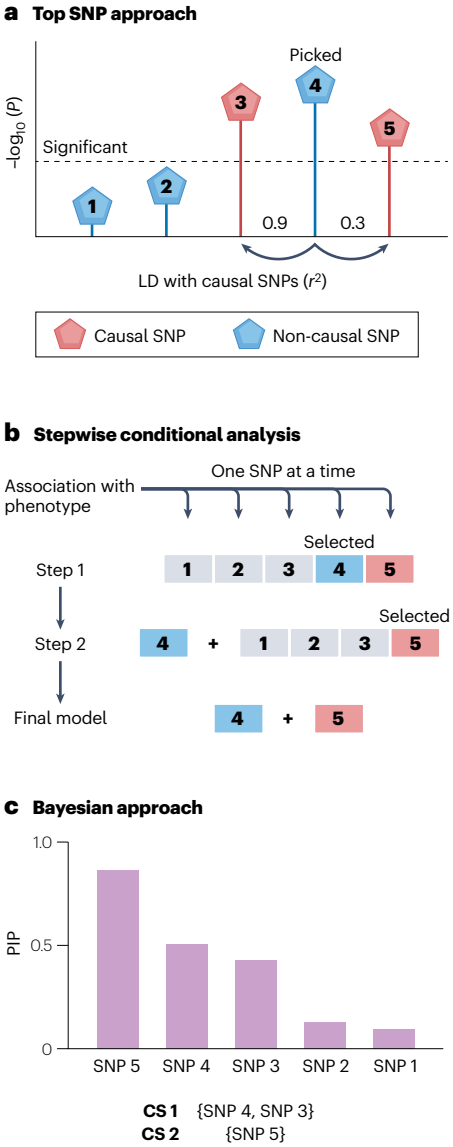

Fig. 1 | Difference in fine-mapping approaches illustrated in a simple scenario. The scenario consists of five SNPs (1, 2, 3, 4 and 5) in a local genomic region in which two SNPs (3 and 5) are causal, whereas the remaining three are non-causal. The non-causal SNP 4 exhibits the strongest marginal *P* value owing to its linkage disequilibrium (LD) with both causal SNPs. **a**, The top SNP approach selects the SNP 4 in the local region with the smallest marginal *P* value. However, this approach is not guaranteed to identify the causal SNP due to stochastic variation or the presence of multiple causal SNPs, as seen in this scenario. **b**, The stepwise conditional analysis sequentially selects SNPs into the model to form a single set, explaining the phenotype association. However, this approach relies on the marginal signals to select initial signals and is sensitive to the order of SNPs examined. In this example, it tests SNPs 1 through 5 one by one in step 1 and selects SNP 4 into the model, as it has the smallest *P* value that passes a pre-specified threshold. In step 2, the approach tests SNPs 1, 2, 3 and 5, one at a time, while conditioning on SNP 4, and selects SNP 5 into the model as it has the smallest conditional *P* value that passes a pre-specified threshold. The algorithm converges after step 2, as none of the remaining SNPs have significant *P* values conditioning on SNPs 4 and 5. As a result, this approach selects one causal SNP 5 and one non-causal SNP 4, while missing the causal SNP 3. **c**, Bayesian fine-mapping approach imposes a sparsity-inducing prior to identify potentially causal SNPs within a likelihood framework. By jointly analysing all SNPs within a locus while accounting for LD, it quantifies the causal probability of each SNP with posterior inclusion probability (PIP) and reports credible sets (CS), each of which contains, with high probability, at least one causal SNP and its correlated non-causal SNPs. For methods based on the SuSiE framework, these PIPs represent the overall PIPs, calculated by aggregating the effect-specific PIPs across all single effects.

Statistical outputs

After the quality control steps, each genomic locus is analysed individually, typically using a Bayesian fine-mapping approach to generate two key statistical outputs for each locus: posterior inclusion probability (PIP), which is given to each variant, and the credible set, which comprises a group of variants. The PIP of a variant represents the posterior probability that the variant is causal given the available data and is a useful metric for prioritizing variants. Unlike marginal *P* values, PIP is typically derived through methods that account for LD within the locus, providing a measure of evidence for causality across different variants in the locus that can be compared across studies[24,27]. The level-ρ credible set, also referred to as the level-ρ confidence set in earlier studies, was originally defined as the smallest set of genetic variants that contains all causal variants with probability ρ or greater[7,17,24,35,36]. ρ is typically set to a large value, such as 95%, to ensure high confidence in including all the causal variants. Fine-mapping approaches using this definition report a single credible set as their output. However, this definition of the credible set is both less informative and less attainable than the one used by recent studies enabled by newer methods.

New definition of credible sets

More recent studies define the level-ρ credible set as the smallest set of genetic variants that contains at least one causal variant with probability ρ or greater[11,19,29]. In contrast to the earlier definition, fine-mapping approaches using this definition report as many credible sets as the data support, with each credible set representing a minimal set of variants that cannot be further disentangled and that contains at least one causal variant[19]. Meanwhile, groups of variants that can be disentangled are assigned to a different credible set, providing additional information for downstream analysis. Importantly, the number of credible sets in the new definition directly reflects the number of causal variants in the locus, whereas, under the earlier definition, this number needs to be inferred as the sum of PIPs of all variants in the credible set, which can be less straightforward[24]. Under the new credible set definition, the number of causal variants must be pre-specified despite being unknown in practice. To ensure that all causal variants are captured, this number is typically set larger than the true number, which in turn leads to the generation of uninformative credible sets — that is, sets composed entirely of non-causal variants. Consequently, post hoc filtering is often necessary to discard uninformative credible set; a commonly used credible set filter is purity, defined as the minimum absolute correlation between all pairs of variants within a credible set[19]. Another, though less commonly used, filter excludes credible sets that do not contain any SNPs with genome-wide significant *P* values from GWAS[12]. However, the mentioned less commonly implemented approach can be overly conservative, as true causal variants may be masked in marginal association analyses[37]. The definitions of PIP and credible set are general and have been adapted to accommodate

scenarios involving functional annotations, multiple traits, multiple genetic ancestries and gene expression studies.

Fine-mapping approaches

Statistical modelling framework

Almost all existing fine-mapping methods build upon a multiple linear regression framework that relates the genotypes within the genomic locus to a phenotype of interest. To introduce this framework, we denote $\boldsymbol{y}$ as the n-vector of phenotypes and denote $\boldsymbol{X}$ as the corresponding n by p genotype matrix for n subjects in GWAS and p SNPs within the locus. Genotypes are typically coded as 0, 1 or 2, or as continuous values ranging from 0 to 2 in the case of imputed genotypes, representing the number of alternative alleles for a given individual. To facilitate computation and simplify notation, we assume that the

Table 1 | Bayesian fine-mapping methods with distinct modelling characteristics

Method	Prior on effect size	Prior on causal configurations	Algorithm	Functional annotation	Multiple ancestries	Multiple traits	TWAS fine-mapping	Summary statistics	Year	Refs.
pi-MASS	Point-normal	Bernoulli-log-uniform	MCMC	No	No	No	No	No	2011	41
CAVIAR CAVIARBF MsCAVIAR	Point-normal	Bernoulli	Exhaustive	No	Yes	No	No	Yes	2014 2015 2021	17,24,36
PAINTOR fastPAINTOR	Point-normal	Bernoulli-logistic	Exhaustive/ Importance sampling	Yes	Yes	Yes	No	Yes	2014 2015 2017	13,35,97
FINEMAP	Point-normal	Bernoulli	SSS	No	No	No	No	Yes	2016	25
JAM	g-prior	Beta-binomial	Exhaustive/ MCMC	No	No	No	No	Yes	2016	42
DAP-G	Point-normal	Bernoulli-logistic	DAP	Yes	No	No	No	Yes	2016 2018	26,47
bfGWAS	Point-normal	Bernoulli-Beta	EM-MCMC	Yes	No	No	No	Yes	2017	78
SuSiE SuSiER	Normal	Multinomial	IBSS	No	No	No	No	Yes	2020 2022	19,30
PolyFun+SuSiE	Normal	Multinomial-discrete	IBSS	Yes	No	No	No	Yes	2020	28
XMAP	Infinitesimal+MVN	Multinomial	VEM	No	Yes	No	No	Yes	2023	57
FiniMOM	Non-local prior	Beta-binomial	MCMC	No	No	No	No	Yes	2023	45
CARMA	Point-normal	Truncated Poisson-logistic	SSS	Yes	No	No	No	Yes	2023	29
SparsePro	Normal	Multinomial-softmax	IBSS	Yes	No	No	No	Yes	2023	50
RSparsePro	Infinitesimal+Normal	Multinomial	IBSS	No	No	No	No	Yes	2024	118
SuSiE-inf	Infinitesimal+Normal	Multinomial	IBSS	No	No	No	No	Yes	2024	49
MESuSiE	Mixture of MVNs	Multinomial	IBSS	No	Yes	No	No	Yes	2024	11
h2-D2	DE-Dirichlet	-	MCMC	No	No	No	No	Yes	2024	44
SuShiE	MVN	Multinomial	IBSS	No	Yes	No	No	Yes	2024	51
MultiSuSiE	MVN	Multinomial	IBSS	No	Yes	No	No	Yes	2024	52
GWFM	Mixture of Normals	Bernoulli-probit	MCMC	Yes	No	No	No	Yes	2024	64
SuSiEx	Normal	Multinomial	IBSS	No	Yes	No	No	Yes	2024	12
SuSiE^2	Normal	Multinomial-discrete	IBSS	Yes	No	No	No	Yes	2024	53
mvSuSiE	Mixture of MVN	Multinomial	IBSS	No	No	Yes	No	Yes	2024	14
FOCUS	Point-normal	Bernoulli	Exhaustive	No	No	No	Yes	Yes	2019	108
MA-FOCUS	Point-normal	Bernoulli	Exhaustive	No	Yes	No	Yes	Yes	2022	109
cTWAS	Normal	Multinomial	IBSS	No	No	No	Yes	Yes	2024	54
TGFM	Normal	Multinomial	IBSS	No	No	No	Yes	Yes	2025	55

DAP, deterministic approximation of posteriors; DE, double exponential; EM-MCMC, expectation-maximization Markov chain Monte Carlo; IBSS, iterative Bayesian stepwise selection; MCMC, Markov chain Monte Carlo; MVN, multivariate normal; SSS, shotgun stochastic search; TWAS, transcriptome-wide association studies; VEM, variational expectation-maximization.

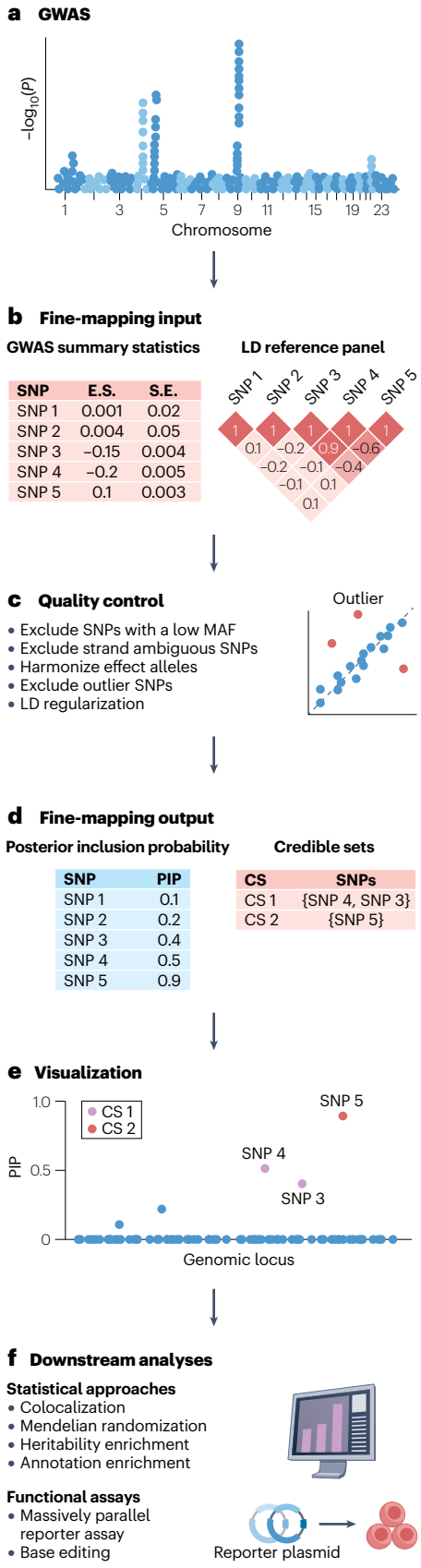

Fig. 2 | A general workflow for fine-mapping analysis with summary statistics. **a**, Genome-wide association studies (GWAS) test for associations between genetic variants and a phenotype of interest. **b**, A typical fine-mapping analysis takes GWAS summary statistics, including effect size estimates (E.S.) and their standard errors (S.E.) from single-variant association analysis, along with an SNP correlation matrix estimated from a reference panel. **c**, Data preprocessing and quality control of the input data, in which MAF represents minor allele frequency. **d**, Fine-mapping analysis outputs the posterior inclusion probability (PIP), which quantifies the causal probability of each SNP, and credible sets (CS), each of which contains, with high probability, at least one causal SNP and its correlated non-causal SNPs. **e**, Visualization of credible set and PIP using a locus zoom plot. **f**, Downstream statistical approaches empirically evaluate the fine-mapping results, whereas functional assays examine the function of the detected SNPs through experimental approaches such as massively parallel reporter assays and base editing. LD, linkage disequilibrium.

phenotype vector $\boldsymbol{y}$ and each column of the genotype matrix $\boldsymbol{X}$ are centred and standardized to have zero mean and unit standard deviation. The multiple linear regression model can then be written as follows:

$$\boldsymbol{y} = \boldsymbol{X}\boldsymbol{\beta} + \boldsymbol{\varepsilon}, \quad (1)$$

in which $\boldsymbol{\beta}$ is a p-vector of SNP effect sizes on the phenotype, and $\boldsymbol{\varepsilon}$ is an n-vector of residual errors with each element assumed to independently and identically follow a normal distribution $N(0, \sigma_\varepsilon^2)$. σ_ε^2 represents the residual variance, typically fixed to be the phenotypic variance (that is, 1) as SNPs within a locus explain only a negligible proportion of variation in the trait[25,30]. Importantly, this multiple regression framework inherently accounts for LD by jointly modelling all SNPs together.

The above linear framework is typically applied to both continuous phenotypes (for example, height, blood pressure or cholesterol levels) or binary phenotypes (for example, presence or absence of a disease). Its application to binary phenotypes is justified, as a linear model serves as an effective first-order Taylor approximation to a generalized linear regression model when SNP effects are small[38]. However, alternative models such as a probit model[39] or logistic model[40], which explicitly account for the binary nature of phenotypes, can be used to improve statistical power.

Despite its simplicity, this model serves as the foundation for almost all existing fine-mapping methods. Within this framework, various fine-mapping methods can be viewed as making distinct modelling assumptions for the genetic effect sizes and relying on different algorithms for identifying the causal SNPs. These methods are typically evaluated using several key strategies (Box 2).

Modelling assumptions for SNP effect sizes

Given that only a small fraction of SNPs in a local region are likely causal, additional modelling assumptions, known as prior assumptions, are necessary for the effect sizes $\boldsymbol{\beta}$ to encourage sparsity and facilitate the identification of causal SNPs. The most commonly used sparse modelling assumption is the spike-and-slab prior, also referred to as the point-normal prior, which assumes that the effect size of SNP j follows $\beta_j \sim \pi N(0, \sigma_\beta^2) + (1-\pi)\delta_0$. The 'slab' component contains π, which represents the probability that the SNP is causal, and N, which denotes that its effect size follows a normal distribution a priori when causal. Notably, the variance σ_β^2 reflects the magnitude of causal effect sizes and is typically either pre-specified based on prior knowledge[24,25,35] or estimated from the data using an empirical

Box 2 | Evaluation of fine-mapping results

Simulation studies, typically designed to closely resemble real data, are widely used to evaluate the performance of fine-mapping methods. Key evaluation metrics in simulations include power, false discovery rate, test statistics calibration and resolution. Power measures the probability of correctly identifying a causal SNP among the true causal variants, whereas false discovery rate quantifies the proportion of non-causal SNPs among those identified, often assessed using posterior inclusion probability thresholds of 0.5 or 0.9. Calibration of test statistics is evaluated at two levels. Calibration of posterior inclusion probability assesses whether the posterior probability of a SNP being causal reflects the truth, whereas calibration of credible set evaluates whether the set contains the intended number of causal variants — for example, a 95% credible set should contain all, or at least one, causal variant with a probability of at least 95%, depending on the credible set definition. Finally, resolution refers to the size of credible sets, with higher resolution indicating smaller sets that facilitate more precise localization of causal variants. Resolution is influenced by factors such as statistical power and the local linkage disequilibrium structure.

In real-data applications, evaluating fine-mapping results is inherently challenging owing to the absence of ground truth. Several empirical evaluation strategies have been proposed, mostly based on enrichment analysis. These include assessing the enrichment of heritability attributable to the identified variants[134,135]; the enrichment of fine-mapped SNPs in functional categories, such as expression quantitative trait loci, missense variants or regulatory elements[11,136]; and concordance with previously reported findings in the literature[11]. These strategies are relatively straightforward to implement and provide indirect but informative evidence for the enrichment of true causal variants in fine-mapping results.

Finally, functional assays such as massively parallel reporter assays (MPRAs)[132] and base editing[133] have been used to experimentally validate fine-mapping results at single-base-pair resolution. Through such functional assays, variants identified as statistically causal through fine-mapping have, in several cases, been validated as likely biologically causal. For example, in a study of blood traits, statistical fine-mapping paired with enhancer activity data identified 543 candidate *cis*-regulatory elements across 254 loci[137]. A follow-up MPRA, STING-seq, was used to perturb each candidate *cis*-regulatory element, successfully linking 134 *cis*-regulatory elements to target genes in a human erythroid progenitor cell line. Direct variant insertion with base editing further tested 46 variants, validating their functional effects at single-base-pair resolution. Importantly, functional assays are typically restricted to model systems, such as cell lines or non-human model organisms, which serve as proxies for human physiology. Consequently, a variant deemed functional in such assays may not necessarily be causal in the relevant tissue in vivo, nor may it completely overlap with variants identified through statistical fine-mapping that are conducted at the population level. For example, a study of psychiatric disorders investigated 683 expression-modulation variants identified by MPRA in a human neural progenitor cell line[138]. Of these, 438 were not included in the credible set of any of three fine-mapping methods — FINEMAP, SuSiE and CAVIAR — whereas 198 were included in the credible set of all three. Notably, in regions with relatively simple linkage disequilibrium structures (in which statistical fine-mapping is most effective) variants identified from statistical fine-mapping tend to modulate expression as determined by MPRAs. Together, these findings highlight the fact that statistical fine-mapping provides informative evidence and can complement functional assays in identifying biologically causal variants.

Bayes approach[19]. Conversely, the 'spike' component contains $1-\pi$, which is the probability that the SNP is non-causal, and δ_0, which denotes that its effect size is zero when non-causal. To facilitate inference in the above model, a p-vector of binary indicators, $\boldsymbol{\gamma}$, is introduced. Each element γ_j takes a value of 1 or 0, indicating whether SNP j is causal or non-causal, respectively. Under the spike-and-slab prior, the causal indicator γ_j follows a Bernoulli distribution, $\gamma_j \sim \text{Bern}(\pi)$. The model defined by equation (1), paired with a spike-and-slab prior on SNP effect sizes, is commonly referred to as the Bayesian variable selection regression[41].

The above model assumes independence in the causal SNP effect sizes, as there is no good reason to believe that the correlation structure of causal effects follows that of the SNPs owing to LD[41]. More specifically, two SNPs are not believed to share a causal status a priori simply because they are in high LD. Despite this independent prior assumption, the posterior estimates of effect sizes remain correlated, as the likelihood in equation (1) accounts for LD. Certainly, the g-prior (that is, a type of prior that induces a priori correlation among SNP effect sizes) can be used instead of the normal prior for the causal effects when there is strong evidence that the correlation structure of causal effects mirrors that of the SNPs[42]. In this case, the causal SNP effect sizes jointly follow $N_{|\boldsymbol{\gamma}|}(0, \sigma_\beta^2(\boldsymbol{X}_\gamma^T\boldsymbol{X}_\gamma)^{-1})$, in which $|\boldsymbol{\gamma}|$ denotes the number of causal SNPs and $\boldsymbol{X}_\gamma$ is the corresponding genotype matrix for these causal SNPs.

The parameter π in the above model represents the proportion of causal SNPs — or equivalently, the prior probability that any given SNP is causal — and is typically assumed to be a small value a priori to encourage sparsity. Some methods fix π to be m/p, in which m denotes the expected number of causal SNPs[17,24,25,36,43]. For example, CAVIARBF[24] and FINEMAP[25] assume $m = 1$, whereas GUESSFM assumes $m = 3$ (ref. 43). Other methods incorporate an additional prior on π to account for its uncertainty. For example, pi-MASS assumes that π follows a uniform prior on the log-scale, $\log(\pi) \sim U(\log(\frac{1}{p}), \log(\frac{m}{p}))$ (default $m = 300$)[41], whereas JAM assumes that π follows a Beta distribution, $\pi \sim \text{Beta}(a, b)$, with weakly informative hyperparameters by setting $a = 1$ and $b = 9$ (ref. 42). Beyond the standard Bernoulli prior on $\boldsymbol{\gamma}$, which is derived from the spike-and-slab prior on $\boldsymbol{\beta}$, CARMA instead models $\boldsymbol{\gamma}$ directly using a truncated Poisson distribution[29].

Moving towards efficient algorithms for model fitting

A key parameter of interest in the above model is the posterior probability of each SNP being causal, denoted as $\Pr(\gamma_j = 1|D)$, in which D represents the data. This metric is known as PIP, as previously mentioned. The simplest approach for posterior inference in the above

model is to use Markov chain Monte Carlo (MCMC), which iteratively updates each parameter conditional on others to produce a sequence of samples that approximate the posterior distribution of $\boldsymbol{\gamma}$[41,42,44,45]. Using these samples, the PIP of each SNP can be estimated by calculating the proportion of posterior samples in which the variant is included as a causal SNP[45]. However, MCMC must explore 2^p causal SNP configurations, making it computationally prohibitive, and it requires a large number of posterior samples for accurate approximation. To improve effective exploration of the causal SNP configuration space, several specific forms of MCMC have been proposed. For example, reversible-jump MCMC[42] proposes new causal configurations by adding, deleting or switching one causal SNP from the current causal configuration, enabling concentrated exploration of likely causal configurations. Similarly, FINEMAP utilizes a shotgun stochastic search algorithm, an iterative procedure designed to effectively explore local causal configurations, enabling it to focus on space enriched with important causal configurations[25].

An alternative approach to MCMC is to exhaustively search the model space and directly evaluate the posterior probability of each causal configuration using the following formula:

$$\Pr(\boldsymbol{\gamma}|D) = \frac{\Pr(\boldsymbol{\gamma})\Pr(D|\boldsymbol{\gamma})}{\sum_{\boldsymbol{\gamma}_c \in \Gamma} \Pr(\boldsymbol{\gamma}_c)\Pr(D|\boldsymbol{\gamma}_c)}. \quad (2)$$

in which the normalizing constant, $\sum_{\boldsymbol{\gamma}_c \in \Gamma} \Pr(\boldsymbol{\gamma}_c)\Pr(D|\boldsymbol{\gamma}_c)$, requires summation over 2^p possible causal configurations, which becomes computationally feasible only if the number of causal SNPs is restricted to a small value. For example, both CAVIAR[17] and PAINTOR[35] set the maximum number of causal SNPs to a small value of k (default, $k = 2$), reducing the causal configuration space from 2^p to $\sum_{i=0}^{k} \binom{p}{i}$, in which $\binom{p}{i}$ denotes the number of ways to select i causal SNPs from a total of p SNPs. Once the posterior probability of each causal configuration is calculated, PIP of each SNP can be computed by marginalizing over all other SNPs in the form of $\Pr(\gamma_j = 1|D) = \sum_{\boldsymbol{\gamma}_c:\gamma_j=1} \Pr(\boldsymbol{\gamma}_c|D)$. Notably, the computation of $\Pr(\boldsymbol{\gamma}|D)$ can be carried out by expressing it in terms of Bayes factors, defined as $\Pr(D|\boldsymbol{\gamma})/\Pr(D|\boldsymbol{\gamma}_0)$, in which $\boldsymbol{\gamma}_0$ denotes the null configuration with no causal SNPs. In the extreme case in which the simplified assumption of a single causal SNP is made (that is, $k = 1$), an approximate Bayes factor (ABF) can be computed directly from GWAS summary statistics without requiring an LD matrix[46]. This ABF, when combined with the assumption that each SNP has an equal prior probability of being causal, yields a simple form of PIP, calculated as $\mathrm{ABF}_j / \sum_{j=1}^{p} \mathrm{ABF}_j$, as adopted in early Bayesian fine-mapping approaches[16]. Nevertheless, this exhaustive search approach remains computationally intensive when the number of causal SNPs k in the genomic locus exceeds a small number.

To further improve computational efficiency, DAP-G[26,47] applies the deterministic approximation of posterior algorithm to first identify sets of high-priority SNPs through a Bayesian version of conditional analysis[48], in which each set is obtained from a conditioning step and contains SNPs that are highly correlated with each other. Subsequently, DAP-G refines the causal configuration space to be all possible combinations that select at most one SNP from each set of high-priority SNPs. By restricting the evaluation space into a smaller set and using it to approximate the normalizing constant, DAP-G further improves computational efficiency. Unlike a standard conditional analysis, DAP-G includes all SNPs with a conditional PIP greater than a predetermined threshold at each step, which avoids the early situation in which only one of two highly correlated SNPs is included.

More recently, variational Bayes algorithms have been proposed to effectively fit the above model[11,12,14,19,49–57]. The main idea behind variational Bayes is to approximate the posterior distribution with a product of simpler functions by minimizing the Kullback–Leibler divergence from the approximation function to the posterior distribution[58]. However, the standard variational Bayes algorithm is ineffective when posterior samples of parameters are highly correlated, as is the case of fine-mapping[59]. To address this issue, the 'sum of single effects' model (SuSiE) has been proposed, which effectively reformulates the above model through re-parameterization to disentangle posterior correlation and re-expresses the genetic effects $\boldsymbol{\beta}$ as a sum of L single effects, such that $\boldsymbol{\beta} = \sum_{l=1}^{L} \boldsymbol{\gamma}_l \beta_l$, in which $\boldsymbol{\gamma}_l$ is a p-dimensional binary indicator vector with only one element equal to one, and the remaining are zeros to represent the l^{th} causal SNP with non-zero effect[19]. L is often set to be a relatively large number (for example, $L = 10$), as fine-mapping results tend to be robust to the over-specification of L, but they can be sensitive to under-specification. The resulting non-informative credible set, owing to the over-specification of L, consists entirely of non-causal variants and can be subsequently removed based on purity. The binary indicator vector $\boldsymbol{\gamma}_l$ is assumed to follow a multinomial distribution, $\boldsymbol{\gamma}_l \sim \mathrm{Multi}(1, \boldsymbol{\pi})$, in which $\boldsymbol{\pi}$ is a p-vector of prior probability for each SNP being causal. In SuSiE, $\boldsymbol{\pi}$ is pre-fixed, with the default setting assigning equal probability to all SNPs (that is, $\pi_j = 1/p$). The non-zero effect for the l^{th} causal SNP, β_l, is assumed to follow a normal distribution with a mean of zero and an effect-specific variance of σ_l^2 that can be estimated from the data using an empirical Bayes approach[19]. This reformulation in SuSiE, paired with the variational Bayes algorithm, naturally leads to a model fitting procedure, referred to as the iterative Bayesian stepwise selection algorithm, that somewhat resembles the stepwise conditional analysis discussed earlier. Briefly, at each step indexed by l, iterative Bayesian stepwise selection aims to identify one causal SNP and its associated effect size by fitting a single-effect regression model[60]. This task is achieved by regressing the residuals $\boldsymbol{y} - \boldsymbol{X}\sum_{l' \neq l} \boldsymbol{\gamma}_{l'}\beta_{l'}$ that exclude the l^{th} single effect, on the genotype matrix $\boldsymbol{X}$. Throughout the iterative process, selections and estimations are continuously re-evaluated until convergence. By assuming that there exists only one causal SNP at each step, SuSiE avoids the complexity of exploring various causal configurations and substantially improves computational efficiency. Importantly, SuSiE is able to quantify the uncertainty about which SNPs to select at each step, enabling it to directly provide multiple credible sets, each aimed at capturing one causal SNP.

The computational cost of fine-mapping varies widely across methods and depends on factors such as sample size (n), the number of SNPs in a region (p), and the assumed maximum number of causal SNPs (k) or single effects (L). Early methods such as CAVIAR and PAINTOR rely on exhaustive search, resulting in polynomial time complexity proportional to p^k, though they scale linearly with n. By prioritizing causal configurations with high posterior probabilities, FINEMAP and DAP-G achieve substantial speedups, improving computation by hundreds to thousands of times. SuSiE offers the most scalable approach to date, with linear computational complexity in n, p and L. In a simulation study with three true causal SNPs, SuSiE was reported to be several times faster than DAP-G, dozens of times faster than FINEMAP and thousands of times faster than CAVIAR[19].

Alternative effect size assumptions and use of GWAS summary statistics

The spike-and-slab prior is the most commonly used prior about SNP effect sizes, but other priors previously used for polygenic score

modelling have been explored for fine-mapping[61]. For example, both SuSiE-inf[49] and XMAP[57] adopt the Bayesian sparse linear mixed model (BSLMM) polygenic assumption[62] about genetic architecture, in which all SNPs are assumed to have at least a small effect, with a small subset exhibiting large effects. Consequently, the goal of fine-mapping shifts towards identifying the subset of SNPs with large effects. By modelling the additional polygenic effects, SuSiE-inf shows improved accuracy[49]. Additionally, genome-wide fine-mapping follows SBayesRC[63] by modelling each causal effect as a mixture of four normal distributions, enabling it to flexibly capture the effect size distributions across a large number of SNPs encountered in genome-wide fine-mapping analysis[64]. By contrast, finiMOM assumes a non-local prior on the causal effect, which differs from a normal distribution in that it has a density value of zero at zero[45]. Finally, h2-D2 makes use of a continuous global-local shrinkage prior that models each element of $\boldsymbol{\beta}$ with a double-exponential distribution whose variance follows a Dirichlet prior[44,65]. Owing to the use of a non-sparse prior, h2-D2 uses a different statistic to PIP in order to assess the causality of each SNP, defined as the difference in posterior probabilities of having positive and negative SNP effect sizes, effectively identifying SNPs whose effect sign can be confidently determined from the data.

Although we have described fine-mapping methods using individual-level data, most of these methods can directly make use of GWAS summary statistics, which facilitates data sharing and computation while ensuring privacy protection[1,2,4]. These summary statistics typically include marginal z-scores for each SNP and the LD matrix, which is often estimated from a reference panel of individuals with the same genetic ancestry[66]. Two primary strategies exist for developing fine-mapping methods that use summary statistics. One strategy involves formulating the model with individual-level data and then substituting the sufficient statistics with summary data[30]. The other strategy directly models summary statistics, bypassing individual-level data[17,35]. A notable drawback of using summary statistics arises when the LD matrix is estimated from a reference panel — even an in-sample panel constructed from randomly selected study samples — as mismatches can still occur, potentially compromising the accuracy and stability of fine-mapping[34].

Incorporating additional information to improve fine-mapping

Beyond what is available in a single GWAS dataset, extensive efforts have been made to develop fine-mapping methods that can incorporate additional sources of information. These include SNP functional annotations, multiple traits, data from diverse genetic ancestries and gene expression studies (Fig. 3). Not only can the incorporation of such information improve the statistical power of fine-mapping methods, but it can also provide key insights into the underlying genetic basis by advancing our understanding of genetic architecture, pleiotropy and gene expression regulation.

SNP functional annotations

A wide range of SNP functional annotations have been collected or constructed from multiple key resources such as the ENCODE[67] and Roadmap Epigenomics project[68]. These annotations capture diverse aspects of variant function, including coding changes, regulatory activity across cell types, evolutionary conservation and pathogenicity. Annotations are provided either as discrete functional groupings, such as missense, synonymous and intergenic, or as quantitative functional scores, such as the 'CADD score'[69] (CADD: combined annotation-dependent depletion). Functional annotations can be retrieved using tools such as VEP[70] and ANNOVAR[71] and have been curated into high-level models such as the baseline-LD and baseline-LF models[72,73]. By leveraging these annotations, functional annotation-informed fine-mapping seeks to further enhance fine-mapping accuracy[26,28,29,32,35,47,50,53,64,74–78] (Fig. 3a).

Two general strategies have been proposed to incorporate functional annotations. One strategy directly models the prior causal probability of each SNP based on its functional annotations. For example, PAINTOR, DAP-G and CARMA use a logistic model, bfGWAS[78] adopts a Beta distribution, GWFM uses a probit model, and SparsePro[50] applies a softmax function. To estimate the effects of functional annotations on causal probability, an expectation-maximization algorithm is commonly used, treating the causal configuration of SNPs as latent variables[79]. The other strategy, exemplified by PolyFun, models the prior causal probability of each SNP as proportional to its per-SNP heritability[28,80], which is further modelled as a weighted sum of SNP functional annotations[81]. PolyFun follows a two-step procedure to first estimate the annotation effects on per-SNP heritability, which is then incorporated into modelling per-SNP causal probability. When a broad set of SNP annotations from curated resources is available, it is often important to infer their relative contributions to fine-mapping, as certain tissues and cell types are more relevant to specific traits than others. For example, kidney-related annotations are particularly informative in the analysis of estimated glomerular filtration rate[50]. Applying regularization to annotation weights, as implemented in methods such as CARMA and PolyFun, can help to prevent model overfitting and to enhance the identification of relevant annotations.

The above methods were designed to incorporate a broad range of functional annotations, whereas SuSiE^2 focuses specifically on integrating gene expression mapping studies into fine-mapping by fitting two SuSiE models[53]. The first model is applied to gene expression mapping studies to identify SNPs associated with gene expression[82]. The PIPs from this model are then used as prior causal probabilities in the second model to identify causal SNPs for the phenotype of interest. This approach effectively assumes that SNPs influencing gene expression levels are more likely to be causal to the phenotype, which enhances fine-mapping power when such assumption holds.

Multi-trait fine-mapping

Many SNPs exhibit pleiotropic effects, influencing multiple biologically relevant complex traits or diseases[83,84]. Consequently, jointly modelling multiple traits through multi-trait fine-mapping approaches can enhance fine-mapping power (Fig. 3b). Several methods have been developed for this purpose, most of which rely on a multivariate linear regression model to account for trait correlations while incorporating distinct assumptions about SNP effects across traits[13,14,85–87]. For example, fastPAINTOR accounts for genetic correlations among traits and assumes that all causal SNPs have non-zero effects on all traits[13]. flashfm further accounts for additional residual correlations owing to shared environmental factors and relaxes the SNP effects assumption by encouraging, but not enforcing, causal SNPs to be sharing across traits[86]. mvSuSiE explicitly models both genetic and residual correlations across traits, and it models each single effect vector using a mixture of multivariate normal distribution to encourage distinct causal SNP sharing patterns across traits, thus further enhancing fine-mapping power[14].

In multi-trait fine-mapping analysis, selecting relevant traits for analysis is a key consideration. Ideally, traits that share substantial underlying genetic architecture provide the greatest benefit, as they

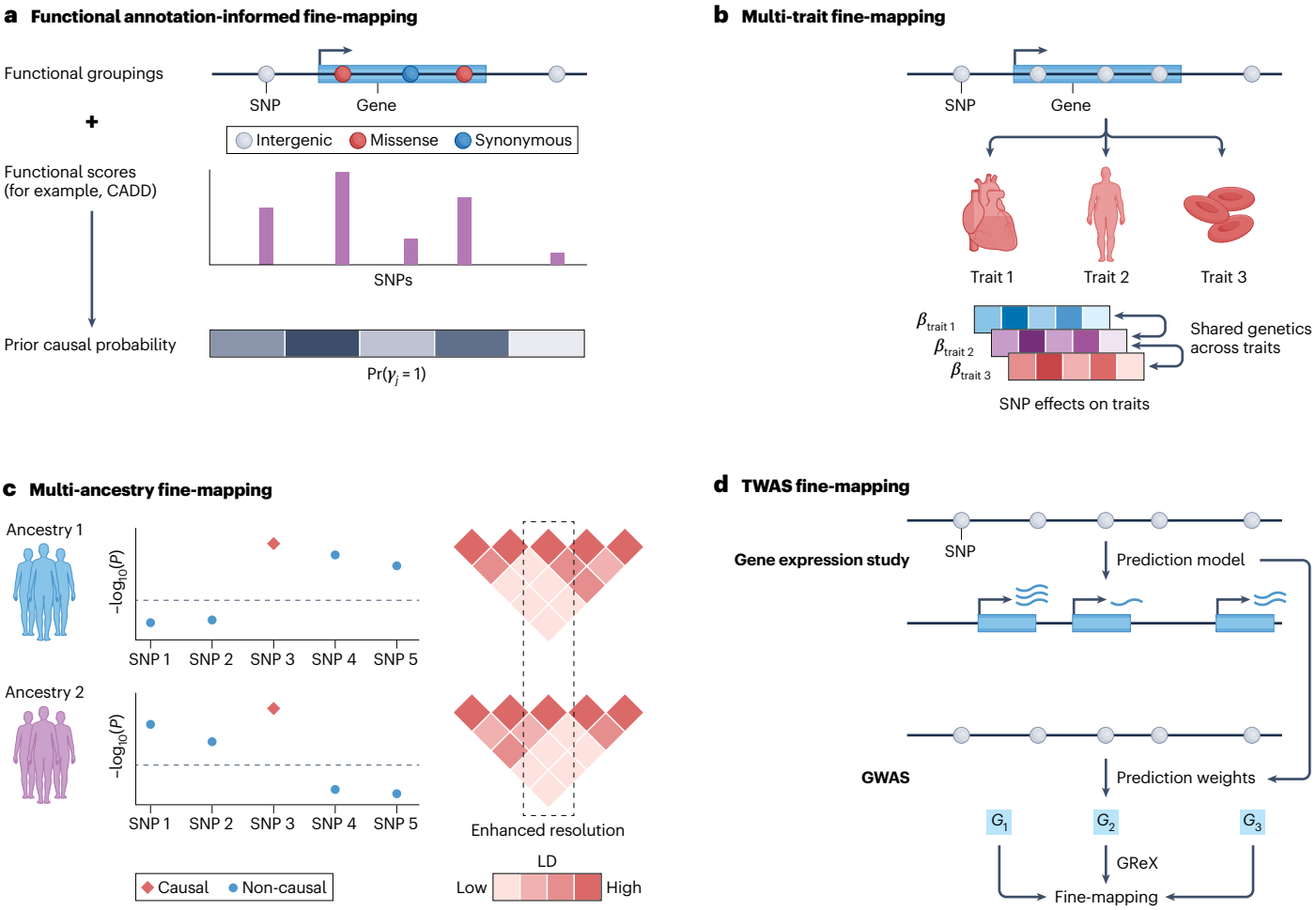

Fig. 3 | Incorporating additional information enhances the power of fine-mapping. a, Functional annotations, in the form of functional groupings or scores, provide valuable information about the causality or effect sizes of SNPs and can thus be incorporated as priors to improve fine-mapping. **b**, Multi-trait fine-mapping leverages shared genetic architecture across traits and explicitly models pleiotropic effects to enhance fine-mapping. **c**, Multi-ancestry fine-mapping uses the shared or ancestry-specific genetic architectures while accounting for distinct linkage disequilibrium (LD) patterns, thereby improving the resolution of fine-mapping across ancestries. **d**, Transcriptome-wide association study (TWAS) fine-mapping integrates a gene expression mapping study with genome-wide association studies (GWAS) to identify potential causal genes for a trait. The gene expression mapping study is used to build expression prediction models in which SNPs serve as predictors of gene expression, and the resulting prediction weights are used to construct genetically regulated expression (GReX) in GWAS. With rare exceptions such as gene-based integrative fine-mapping through conditional TWAS (GIFT), TWAS fine-mapping typically uses the same modelling framework as GWAS fine-mapping, substituting SNP genotypes with GReX as exposure variables. CADD, combined annotation-dependent depletion.

are more likely to share the same causal variants. Several strategies have been proposed for trait selection, including those based on prior biological or clinical knowledge[14,85,86], the presence of pleiotropic GWAS signals[13], or the significance of genetic correlations[88]. In principle, including more genetically correlated traits can improve fine-mapping resolution and enhance the power to detect causal variants; however, in practice, modelling more traits increases the computational burden and number of parameters to the model, which could reduce power, especially for causal variants that affect only a subset of traits.

When focusing on two traits — one being a complex trait of interest and the other a molecular trait such as the expression level of a specific gene — the multi-trait fine-mapping becomes closely related to colocalization analysis, which aims to evaluate the genetic relationship between two traits by assessing whether they share the same causal variants at a given locus[89]. Both analyses rely on similar underlying statistical models, with colocalization analysis summarizing results using posterior probabilities that both traits are associated with the same causal variant, a quantity closely related to PIP in fine-mapping settings. For example, eCAVIAR builds upon the CAVAIR framework to estimate the probability that a variant is causal for both a GWAS trait and gene expression[90]. SuSiE-coloc directly uses fine-mapping results from SuSiE and applies coloc to assess colocalization of each pair of credible sets from the two traits[91]. Additionally, multi-trait fine-mapping methods such as mvSuSiE extend traditional fine-mapping by explicitly modelling genetic correlation across traits, offering insights into the extent of shared versus trait-specific genetic effects — a related goal of colocalization[14].

Multi-ancestry fine-mapping

The increasing availability of GWAS data obtained in consortium studies across multiple genetic ancestries, such as All of Us[92], Biobank Japan[93] and UK Biobank[94], presents a unique opportunity to enhance fine-mapping analysis[95]. Two naive fine-mapping approaches were used early on to leverage GWAS data from multiple ancestries: the first meta-analyses GWAS summary statistics across ancestries before fine-mapping, and the second fine-maps each ancestry separately and then post-processes the results to identify shared or ancestry-specific causal variants[11,12]. However, these naive strategies fail to fully take advantage of the shared and ancestry-specific components of the genetic architecture and do not account for differences in power across ancestries owing to varying sample sizes. As a result, they can lead to miscalibration of test statistics and reduced fine-mapping power.

Multi-ancestry fine-mapping approaches have been recently developed to explicitly leverage the shared genetic architecture[96] while accounting for differences in LD patterns across ancestries[11,12,36,51,52,57,97–99] (Fig. 3c). Most of these methods are built on the SuSiE framework and differ mainly in their modelling assumptions about the causal SNP effect sizes across ancestries. Specifically, SuSiEx assumes that all causal SNPs are shared across ancestries and that their effect sizes are uncorrelated across ancestries a priori[12]. By contrast, MultiSuSiE[52] and SuShiE[51] relax this assumption: although both methods still assume that the causal SNPs are shared across ancestries, they allow for the effect sizes to be correlated across ancestries by using a multivariate normal distribution. Despite their similar modelling assumptions, MultiSuSiE was primarily applied to fine-mapping causal variants in GWAS whereas SuShiE was primarily applied to fine-mapping *cis*-molecular quantitative trait loci in functional genomics studies[100–102]. Finally, MESuSiE introduces more flexible modelling assumptions by allowing some causal SNPs to be shared across ancestries and others to be ancestry-specific[11]. This feature is achieved by introducing a binary indicator vector for each causal SNP, in which each element represents whether the SNP is causal in a particular ancestry or shared across ancestries, and further modelling their effect size correlation across ancestries with a multivariate normal distribution. Not only does such flexibility in modelling by MESuSiE enhance fine-mapping resolution across ancestries, but it also facilitates the characterization of both shared and ancestry-specific genetic architectures[96,103].

TWAS fine-mapping

Several techniques originally designed for fine-mapping causal variants in GWAS have been recently adapted to fine-map causal genes through transcriptome-wide association studies (TWAS)[104–106]. TWAS integrates GWAS with gene expression studies to identify genes whose genetically regulated expression (GReX) is associated with a trait of interest, revealing regulatory mechanisms underlying complex traits and diseases. A typical TWAS involves two analytic stages. In the first stage, TWAS builds expression prediction models in the expression study in which SNPs are used to predict gene expression. In the second stage, TWAS uses the estimated SNP prediction weights to construct GReX in the GWAS and tests the association of GReX with the trait.

Given that genes within the same genomic locus may have correlated expression values or contain expression quantitative trait loci that are in LD with each other, many genes identified in TWAS may represent tagging genes rather than causal ones[107]. To narrow down the list of potential causal genes, several TWAS fine-mapping approaches have been proposed[20,54,55,108,109] (Fig. 3d). Most of these methods adopt techniques originally designed for fine-mapping causal variants in GWAS, effectively replacing SNPs with GReX for genes located within the genomic locus. For example, FOCUS adapts Bayesian variable selection regression with an exhaustive search algorithm to fine-map TWAS associations[108]. cTWAS extends SuSiE towards TWAS fine-mapping while controlling for SNP horizontal pleiotropic effects[54]. In contrast to these approaches that directly adapt GWAS fine-mapping for TWAS fine-mapping, GIFT (gene-based integrative fine-mapping through conditional TWAS) takes a frequentist approach[20] by recognizing that the number of genes per region is often much smaller than the number of SNPs, and therefore the complex apparatus developed for GWAS fine-mapping may not be necessary for TWAS fine-mapping. Specifically, GIFT conducts conditional analysis within the local region, focusing on testing one gene at a time while conditioning on all other genes in the region. Although the above methods focus on integrating gene expression data from a single tissue, another tool, TGFM, further presents cross-tissue TWAS fine-mapping by leveraging gene expression data from multiple tissues[55]. By constructing GReX across multiple tissues, TGFM jointly fine-maps causal gene–tissue pairs and non-mediated genetic variants, facilitating the identification of both causal genes and their tissues of action. Importantly, the power of TWAS fine-mapping methods is often constrained by the limited sample size of gene expression study — a limitation that is expected to diminish as larger expression quantitative trait loci mapping studies become available over time.

Remaining challenges

With the goal of improving the power, resolution and scalability of statistical fine-mapping, several challenges lie ahead. Central to these challenges is model misspecification, which arises when the model used to fit the data deviates from the true data-generating process that is inherently unknown in real-data applications. Model misspecification in fine-mapping can stem from multiple sources. First, all current fine-mapping methods assume a linear additive genetic model to describe the relationship between genotype and trait. Although both theoretical exploration and empirical evidence suggest that additive effects account for the majority of genetic variation in complex traits[110,111], non-additive and nonlinear effects — such as dominance, epistasis, gene–environment interactions and haplotypic effects (especially those not well tagged by a linear combination of SNPs) — may also contribute to trait variation and influence the identification of causal variants for particular traits or at specific loci[112,113]. Second, existing fine-mapping methods typically account for population stratification using genetic principal components[114] or additional random effects terms[115]. These approaches are often effective in the presence of discrete ancestries or subtle structures, but they may fail to fully control for complex population structures, particularly in admixed populations, leading to residual confounding that affects both the accuracy and the causal interpretation of fine-mapping results[116]. In addition to these modelling issues, further sources of misspecification are addressed in detail below.

Miscalibration of fine-mapping with summary statistics

Many fine-mapping methods directly use summary statistics, which rely on two implicit but critical assumptions: first, that the marginal *z*-scores across SNPs are correctly calculated, and, second, that the SNP LD matrix inferred from the reference panel matches the data from which the *z*-scores were derived. However, both assumptions may fail in real-world applications. Specifically, the marginal *z*-scores

are often obtained from GWAS meta-analysis in consortium studies, in which inter-cohort heterogeneity, if not well adjusted for, can lead to miscalculation of the marginal *z*-scores or mismatch between the *z*-scores and the LD matrix, resulting in false positives and miscalibration in the subsequent fine-mapping analysis[34] (Fig. 4a). Some of this inter-cohort heterogeneity is biological, including population-specific effects from SNPs, gene–gene interactions and gene–environment interactions. Other sources of heterogeneity are technical, including variations in phenotyping criteria or measurement protocols, genotyping arrays, imputation panels, quality control criteria and analytical software, all of which can contribute to increased miscalibration of PIP or credible set in fine-mapping. Additionally, small sample sizes in the reference data can introduce variability in the estimated LD matrix, and mismatches in ancestry between the reference and the study data may also lead to bias in the LD matrix, resulting in its mismatch with *z*-scores[30,117].

Several methods have been developed to detect outlier SNPs whose summary statistics may not match the LD reference due to inter-cohort heterogeneity or mismatched reference data. Specifically, DENTIST[33] and SuSiER (with the kriging_rss function)[30] assume that the effect of any single SNP is negligible. Under this assumption, the expected marginal *z*-score of each SNP can be computed based on the *z*-scores of all other SNPs in the locus with LD, which is then compared with the observed *z*-scores to detect outlier SNPs (Fig. 4b). SuSiER further regulates the LD matrix (with the estimate_s_rss function), with the regularization parameter estimated from the observed *z*-scores. By contrast, SLALOM assumes that the lead PIP SNP in a locus is the only causal variant, enabling it to examine the association statistics of neighbouring SNPs for deviations from expected LD-based relationships using a modified DENTIST-S statistic[34]. The lead PIP variants in the flagged suspicious loci are often depleted for likely causal variants, highlighting the effectiveness of SLALOM. CARMA integrates a Bayesian procedure into its algorithm for detecting and removing outlier SNPs, again by leveraging deviations in association statistics from expected LD-based relationships, ensuring that only the LD relationships among the estimated causal SNPs are evaluated. Finally, rather than removing outlier SNPs, RSparsePro directly accounts for LD mismatch in fine-mapping by modelling the observed *z*-scores ($\hat{\boldsymbol{z}}$) as error-contaminated observations of latent *z*-scores ($\boldsymbol{z}$), assuming $\hat{\boldsymbol{z}} \sim N(\boldsymbol{z}, \sigma_s^2 \boldsymbol{I})$, with the variance parameter σ_s^2 quantifying the extent of discrepancy owing to LD mismatch[118]. Despite the effectiveness of these methods, fine-mapping with summary statistics may still fail in certain genomic loci for specific traits, highlighting the need for further research to fully understand and address this issue.

Missed causal variants

Several factors during quality control can result in the omission of variants in fine-mapping analysis. These factors include the exclusion of variants with low MAF or poor imputation quality, as well as the loss of variants during data harmonization, as only SNPs shared across all studies are retained and analysed[11]. For example, a variant may be missing if it has a low MAF or is poorly imputed in one study or ancestry group but not another, leading to its exclusion from the fine-mapping analysis. Additionally, owing to the small sample size and population difference in the LD reference panel, variants present in GWAS may not necessarily exist in the LD reference panel. Although missing non-causal variants often has little impact, or may even improve the resolution, missing causal variants prevents them from being detected in the credible set and leads to PIPs that no longer reflect the true probability of causality[11]. As such, caution is warranted when interpreting the fine-mapping results.

Fine-mapping rare variants

The study of rare genetic variants, typically defined by having an MAF <1%, is crucial for several reasons. Compared with common variants, rare variants tend to have larger effect sizes[119,120] and are more likely to be functionally important[121]. Recent advances have enabled more effective analysis of individual rare variants in larger cohorts. For example, one study constructed a within-cohort imputation reference panel using whole genome sequencing data from a subset of UK Biobank participants, enabling rare variants to be imputed into array-genotyped samples with substantially improved accuracy[122]. Existing fine-mapping methods can, in principle, be applied to fine-map rare variants, which often exhibit weaker LD that may aid in resolving causal signals. However, their low allele frequency poses a notable challenge to attaining the required statistical power. As a result, fine-mapping outputs such

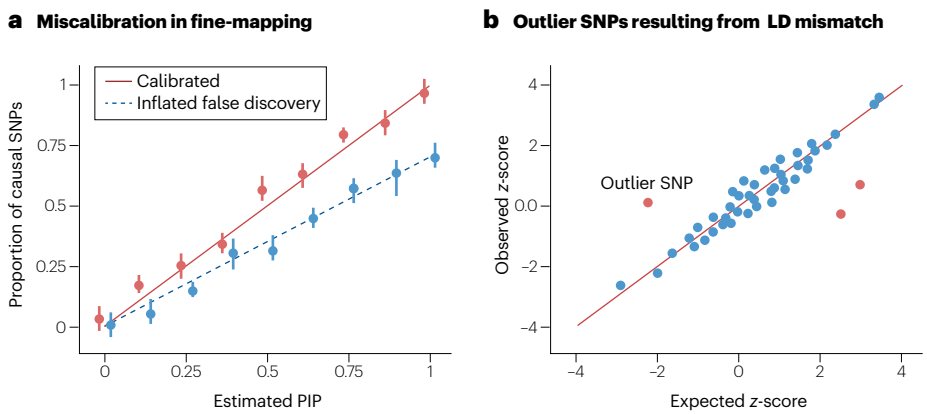

Fig. 4 | Analytic challenges in statistical fine-mapping. a, An example of model miscalibration in fine-mapping in which the estimated posterior inclusion probability (PIP; *x* axis) is higher than the observed proportion of causal SNPs (*y* axis), suggesting a higher false discovery rate than expected. Variants are grouped into nine equally spaced bins based on PIP, with the average PIP and proportion of causal SNPs computed for each bin. **b**, Scatter plot illustrating the relationship between the observed *z*-score and the expected *z*-score across SNPs, given the linkage disequilibrium (LD) matrix estimated from a reference panel and the *z*-scores of neighbouring SNPs. Large deviations between the two values indicate potential mismatch between the *z*-scores and the LD matrix.

Glossary

Bayes factors
Relative marginal likelihood of the observed data under one hypothesis compared with another, often quantifying the evidence in favour of an association versus no association.

Bayesian framework
A statistical framework that represents uncertainty in model parameters using probability distributions; it combines prior beliefs with observed data through Bayes' theorem to compute posterior distributions.

Bernoulli distribution
A discrete probability distribution for binary data that describes the probability of an event with only two possible outcomes, coded as 1 for success and 0 for failure.

Causal configurations
Specific combinations of causal statuses across SNPs within a genomic locus.

Confounding factors
Variables that influence both the outcome and the explanatory variable, leading to spurious associations between outcome and explanatory variable themselves.

Density value
The value of the probability density function evaluated at a given point, capturing the relative possibility for a continuous random variable being near that point.

Double-exponential distribution
Also known as Laplace distribution, it is a continuous probability distribution that resembles the normal distribution but with a sharper peak at the centre and heavier tails to encourage sparsity.

Expectation-maximization algorithm
An iterative algorithm to find maximum likelihood estimates in models with latent or missing variables by alternating between expectation and maximization steps.

Expression quantitative trait loci
Genomic loci in which genetic variants are associated with gene expression levels.

First-order Taylor approximation
A linear approximation of a function based on its value and first-order derivative at a given point.

Generalized linear regression
A generalization of linear regression that relates the linear combination of explanatory variables to the outcome variable through a link function, allowing for different types of outcome variables (for example, counts, binary).

Global-local shrinkage prior
A type of Bayesian prior that incorporates a global parameter to impose overall shrinkage of SNP effect sizes towards zero, while using local parameters to allow SNP-specific adaptive shrinkage of individual effect sizes.

Kullback–Leibler divergence
A measure of the difference between two probability distributions, often used to assess how one distribution diverges from another distribution.

Linkage disequilibrium
(LD). The nonrandom association of alleles at different loci.

Logistic model
A type of generalized linear regression used for binary outcomes in which the log-odds of a binary outcome is modelled as a linear combination of explanatory variables.

Marginal *P* values
In genome-wide association studies, a marginal *P* value refers to the quantification of statistical evidence for an association between a single genetic variant and the phenotype, without accounting for the effects of other variants.

Meta-analysis
A statistical analysis that combines results from multiple studies to reach a single conclusion about a common research question.

Minor allele frequency
(MAF). The frequency of the less common allele at a genetic locus in a population.

Model space
The set of all possible causal configurations within the fine-mapping model.

Multiple linear regression
A regression analysis that models a continuous outcome variable as a linear combination of multiple explanatory variables.

Per-SNP heritability
The proportion of phenotypic variance explained by a single SNP.

Phenotype residuals
The portion of phenotypic variation that remains after accounting for the effects of known covariates in a statistical model; calculated as the difference between observed and model-predicted phenotype values.

Pleiotropy
A genetic phenomenon in which one gene affects multiple traits or diseases.

Poisson distribution
A discrete probability distribution for count data that expresses the probability of a given number of events occurring in a fixed interval of time.

Posterior distribution
The probability distribution of a model parameter given the observed data and prior information.

Posterior probability
The probability of an event given the observed data and prior information.

Probit model
A type of generalized linear regression used for binary outcomes in which the probability of success is modelled using the cumulative distribution function of the standard normal distribution.

Regression
A statistical analysis that estimates the relationship between an outcome variable and one or more explanatory variables.

Regularization
In the context of covariance matrix estimation, regularization refers to the technique of adjusting the sample covariance matrix, typically by adding a multiply of the identity matrix, to ensure invertibility and improve numerical stability.

Statistical power
The probability that a statistical test will correctly detect an effect if it truly exists.

Summary statistics
Effect size estimates and their standard errors from single-variant association analysis in genome-wide association studies, along with an SNP–SNP correlation matrix typically estimated from a reference panel.

as credible set may still be valuable for capturing and summarizing rare variant signals. Additionally, aggregation approaches commonly used in marginal rare variant analysis, such as the burden test[123] or sequence kernel association test[124], can potentially be incorporated into fine-mapping frameworks to assess the combined effect of variant sets, albeit at the cost of reduced mapping resolution. Evaluating

and potentially extending existing fine-mapping methods to better accommodate rare variants represent an important direction for future research.

High replication failure rate

Model misspecifications can have important consequences in real-data applications, contributing to observed high replication failure rate (RFR). RFR, defined as the proportion of high-confidence variants (PIP > 0.9) fine-mapped in a subsample analysis that fail to replicate (PIP < 0.1) in the full sample analysis, has been reported to be inflated in fine-mapping of real data[49]. RFR is an approximate lower bound for the false discovery rate, and an inflated RFR likely reflects a miscalibration in PIP, in which the proportion of truly causal SNPs is lower than that indicated by PIP (Fig. 4a). RFR does not seem to be inflated by factors such as missing causal variants owing to quality control, deviation of effect size distributions from normality and imputation noise, but an important contributor to RFR inflation is the presence of non-sparse genetic architecture, in which many SNPs have small effects. Consequently, methods building upon the BSLMM assumption, such as SuSiE-inf, improve RFR inflation. However, adopting the BSLMM assumption does not fully resolve the high RFR issue, suggesting that additional sources of model misspecification remain.

Conclusion and future perspectives

In this Review, we have discussed advances and challenges in the development of statistical fine-mapping approaches. Our discussion is centred around a multiple regression framework, highlighting various modelling assumptions and numerical algorithms. Additionally, we have examined key challenges in fine-mapping analyses and potential solutions that have been proposed. Beyond causal variant identification, fine-mapping results also facilitate various other statistical analyses, such as colocalization[89] and Mendelian randomization[125]. For example, fine-mapping of the trait and gene expression separately generates credible sets of candidate causal SNPs for each, which can then be used as input for coloc to perform focused colocalization analysis[91]. Similarly, the candidate causal SNPs identified through fine-mapping can serve as instrumental variables for Mendelian randomization, facilitating the investigation of causal relationships between traits[126].

Several future directions hold promises for advancing fine-mapping methodologies, including expanding to new application areas, improving model assumptions and addressing model misspecification. One such direction is fine-mapping in admixed populations, whose genomes consist of a mosaic of segments derived from multiple genetic ancestries. Admixed populations provide unique opportunities to refine fine-mapping resolution by leveraging differences in LD patterns while mitigating confounding from environmental factors[127]. As a recent method to address this topic, CARMA-X leverages local ancestry inference to decompose the genotype matrix of admixed individuals into ancestry-specific components and jointly models the genetic effects across all ancestral components while properly accounting for cross-ancestry LD correlations[116]. Besides stratifying individuals into discrete ancestry groups, developing methods that account for genetic ancestry as a continuum represents an important area for further exploration[128]. Additionally, when integrating information from multiple sources, the type of information that provides the greatest benefit for fine-mapping likely varies across traits and loci. For example, multi-ancestry fine-mapping may be particularly powerful when causal variants are shared across ancestries but exhibit different patterns of LD with neighbouring variants. By contrast, functional annotations are especially valuable in regions with complex LD or when causal variants have functional effects that can be captured by regulatory or epigenomic features. Quantifying the relative contribution of each type of information remains an important future direction. Moreover, most fine-mapping studies have been carried out for mapping the genetic main effects on the trait, implicitly assuming a constant effect size across diverse environmental contexts. However, this traditional approach overlooks an important aspect of genetic influence — genetic effects can be context-dependent and can be modulated by environmental factors[129]. Indeed, both genetic and environmental factors are major contributors to phenotypic variation, and their interactions play a pivotal role in shaping complex traits[130]. Therefore, developing methods towards fine-mapping gene–environment interactions is an important future direction towards uncovering context-specific genetic effects and generating deeper insights into the architecture of complex traits. Finally, with the rapid advancement of deep learning and genome language models[131], investigating how these powerful tools can be integrated to enhance fine-mapping accuracy and interpretability remains a crucial avenue for future research.

Published online: 28 July 2025

References

1. Visscher, P. M. et al. 10 years of GWAS discovery: biology, function, and translation. *Am. J. Hum. Genet.* **101**, 5–22 (2017).
2. Uffelmann, E. et al. Genome-wide association studies. *Nat. Rev. Methods Primers* **1**, 59 (2021).
3. Sollis, E. et al. The NHGRI-EBI GWAS Catalog: knowledgebase and deposition resource. *Nucleic Acids Res.* **51**, D977–D985 (2023).
4. Loos, R. J. F. 15 years of genome-wide association studies and no signs of slowing down. *Nat. Commun.* **11**, 5900 (2020).
5. Wall, J. D. & Pritchard, J. K. Haplotype blocks and linkage disequilibrium in the human genome. *Nat. Rev. Genet.* **4**, 587–597 (2003).
6. Spain, S. L. & Barrett, J. C. Strategies for fine-mapping complex traits. *Hum. Mol. Genet.* **24**, R111–R119 (2015).
7. Schaid, D. J., Chen, W. & Larson, N. B. From genome-wide associations to candidate causal variants by statistical fine-mapping. *Nat. Rev. Genet.* **19**, 491–504 (2018).
8. Broekema, R. V., Bakker, O. B. & Jonkers, I. H. A practical view of fine-mapping and gene prioritization in the post-genome-wide association era. *Open Biol.* **10**, 190221 (2020).
9. Hutchinson, A., Asimit, J. & Wallace, C. Fine-mapping genetic associations. *Hum. Mol. Genet.* **29**, R81–R88 (2020).
10. Wang, Q. S. & Huang, H. Methods for statistical fine-mapping and their applications to auto-immune diseases. *Semin. Immunopathol.* **44**, 101–113 (2022).
11. Gao, B. & Zhou, X. MESuSiE enables scalable and powerful multi-ancestry fine-mapping of causal variants in genome-wide association studies. *Nat. Genet.* **56**, 170–179 (2024).
This paper proposes a multi-ancestry fine-mapping framework that explicitly models both shared and ancestry-specific causal variants, leading to improved accuracy and resolution of fine-mapping.
12. Yuan, K. et al. Fine-mapping across diverse ancestries drives the discovery of putative causal variants underlying human complex traits and diseases. *Nat. Genet.* **56**, 1841–1850 (2024).
13. Kichaev, G. et al. Improved methods for multi-trait fine mapping of pleiotropic risk loci. *Bioinformatics* **33**, 248–255 (2017).
14. Zou, Y., Carbonetto, P., Xie, D., Wang, G. & Stephens, M. Fast and flexible joint fine-mapping of multiple traits via the sum of single effects model. Preprint at *bioRxiv* https://doi.org/10.1101/2023.04.14.536893 (2024).
15. Kachuri, L. et al. Principles and methods for transferring polygenic risk scores across global populations. *Nat. Rev. Genet.* **25**, 8–25 (2024).
16. Wellcome Trust Case Control Consortium et al. Bayesian refinement of association signals for 14 loci in 3 common diseases. *Nat. Genet.* **44**, 1294–1301 (2012).
17. Hormozdiari, F., Kostem, E., Kang, E. Y., Pasaniuc, B. & Eskin, E. Identifying causal variants at loci with multiple signals of association. *Genetics* **198**, 497–508 (2014).
18. van de Bunt, M. et al. Evaluating the performance of fine-mapping strategies at common variant GWAS loci. *PLoS Genet.* **11**, e1005535 (2015).
19. Wang, G., Sarkar, A., Carbonetto, P. & Stephens, M. A simple new approach to variable selection in regression, with application to genetic fine mapping. *J. R. Stat. Soc. B* **82**, 1273–1300 (2020).
This paper proposes a seminal statistical framework — the 'sum of single effects' model, called SuSiE — for fine-mapping that benefits both accuracy and computational efficiency.

20. Liu, L. et al. Conditional transcriptome-wide association study for fine-mapping candidate causal genes. *Nat. Genet.* **56**, 348–356 (2024).
This paper proposes a frequentist TWAS fine-mapping method that leverages the relatively small number of genes within each locus to systematically fine-map causal genes by conditioning on all other genes in the region.
21. Yang, J. et al. Conditional and joint multiple-SNP analysis of GWAS summary statistics identifies additional variants influencing complex traits. *Nat. Genet.* **44**, 369–375 (2012).
22. Keaton, J. M. et al. Genome-wide analysis in over 1 million individuals of European ancestry yields improved polygenic risk scores for blood pressure traits. *Nat. Genet.* **56**, 778–791 (2024).
23. Weng, L. C. et al. The impact of common and rare genetic variants on bradyarrhythmia development. *Nat. Genet.* **57**, 53–64 (2025).
24. Chen, W. et al. Fine mapping causal variants with an approximate Bayesian method using marginal test statistics. *Genetics* **200**, 719–736 (2015).
25. Benner, C. et al. FINEMAP: efficient variable selection using summary data from genome-wide association studies. *Bioinformatics* **32**, 1493–1501 (2016).
This paper proposes a shotgun stochastic search algorithm for fine-mapping that substantially improves computational efficiency, enabling the exploration of configurations with more than a few causal variants.
26. Wen, X., Lee, Y., Luca, F. & Pique-Regi, R. Efficient integrative multi-SNP association analysis via deterministic approximation of posteriors. *Am. J. Hum. Genet.* **98**, 1114–1129 (2016).
This paper proposes a deterministic approximation of posteriors algorithm for fine-mapping that enables highly scalable and accurate identification of causal variants.
27. Stephens, M. & Balding, D. J. Bayesian statistical methods for genetic association studies. *Nat. Rev. Genet.* **10**, 681–690 (2009).
28. Weissbrod, O. et al. Functionally informed fine-mapping and polygenic localization of complex trait heritability. *Nat. Genet.* **52**, 1355–1363 (2020).
This paper proposes a statistical framework that leverages genome-wide functional annotations by coupling an extended version of stratified LD score regression with existing fine-mapping methods, leading to substantially improved fine-mapping power.
29. Yang, Z. K. et al. CARMA is a new Bayesian model for fine-mapping in genome-wide association meta-analyses. *Nat. Genet.* **55**, 1057–1065 (2023).
30. Zou, Y., Carbonetto, P., Wang, G. & Stephens, M. Fine-mapping from summary data with the "Sum of Single Effects" model. *PLoS Genet.* **18**, e1010299 (2022).
This paper systematically investigates summary statistics-based fine-mapping, presenting a generic strategy for extending methods to summary data, diagnostic tools for identifying inconsistencies and approaches for improving summary data consistency.
31. Wu, T. T., Chen, Y. F., Hastie, T., Sobel, E. & Lange, K. Genome-wide association analysis by lasso penalized logistic regression. *Bioinformatics* **25**, 714–721 (2009).
32. Fisher, V., Sebastiani, P., Cupples, L. A. & Liu, C. T. ANNORE: genetic fine-mapping with functional annotation. *Hum. Mol. Genet.* **31**, 32–40 (2022).
33. Chen, W. et al. Improved analyses of GWAS summary statistics by reducing data heterogeneity and errors. *Nat. Commun.* **12**, 7117 (2021).
34. Kanai, M. et al. Meta-analysis fine-mapping is often miscalibrated at single-variant resolution. *Cell Genom.* **2**, 100210 (2022).
This paper demonstrates that the inter-cohort heterogeneity from multiple sources can impair the calibration of fine-mapping when using summary statistics from GWAS meta-analyses, and proposes a quality control method — SLALOM — to mitigate this issue.
35. Kichaev, G. et al. Integrating functional data to prioritize causal variants in statistical fine-mapping studies. *PLoS Genet.* **10**, e1004722 (2014).
36. LaPierre, N. et al. Identifying causal variants by fine mapping across multiple studies. *PLoS Genet.* **17**, e1009733 (2021).
37. Li, A. et al. mBAT-combo: a more powerful test to detect gene-trait associations from GWAS data. *Am. J. Hum. Genet.* **110**, 30–43 (2023).
38. Pirinen, M., Donnelly, P. & Spencer, C. C. A. Efficient computation with a linear mixed model on large-scale data sets with applications to genetic studies. *Ann. Appl. Stat.* **7**, 369–390 (2013).
39. Zhang, H., He, K., Li, Z., Tsoi, L. C. & Zhou, X. FABIO: TWAS fine-mapping to prioritize causal genes for binary traits. *PLoS Genet.* **20**, e1011503 (2024).
40. Zhou, W. et al. Efficiently controlling for case-control imbalance and sample relatedness in large-scale genetic association studies. *Nat. Genet.* **50**, 1335–1341 (2018).
41. Guan, Y. T. & Stephens, M. Bayesian variable selection regression for genome-wide association studies and other large-scale problems. *Ann. Appl. Stat.* **5**, 1780–1815 (2011).
This paper represents one of the earliest work that applies the Bayesian variable selection regression for fine-mapping and underlies many of the following developments.
42. Newcombe, P. J., Conti, D. V. & Richardson, S. JAM: a scalable Bayesian framework for joint analysis of marginal SNP effects. *Genet. Epidemiol.* **40**, 188–201 (2016).
43. Wallace, C. et al. Dissection of a complex disease susceptibility region using a Bayesian stochastic search approach to fine mapping. *PLoS Genet.* **11**, e1005272 (2015).
44. Li, X., Sham, P. C. & Zhang, Y. D. A Bayesian fine-mapping model using a continuous global-local shrinkage prior with applications in prostate cancer analysis. *Am. J. Hum. Genet.* **111**, 213–226 (2024).
45. Karhunen, V., Launonen, I., Jarvelin, M. R., Sebert, S. & Sillanpaa, M. J. Genetic fine-mapping from summary data using a nonlocal prior improves the detection of multiple causal variants. *Bioinformatics* **39**, btad396 (2023).
46. Wakefield, J. Bayes factors for genome-wide association studies: comparison with *P*-values. *Genet. Epidemiol.* **33**, 79–86 (2009).
47. Lee, Y., Luca, F., Pique-Regi, R. & Wen, X. Bayesian multi-SNP genetic association analysis: control of FDR and use of summary statistics. Preprint at *bioRxiv* https://doi.org/10.1101/316471 (2018).
48. Flutre, T., Wen, X. Q., Pritchard, J. & Stephens, M. A statistical framework for joint eQTL analysis in multiple tissues. *PLoS Genet.* **9**, e1003486 (2013).
49. Cui, R. et al. Improving fine-mapping by modeling infinitesimal effects. *Nat. Genet.* **56**, 162–169 (2024).
This paper proposes a fine-mapping method that relies on a SuSiE-based variational algorithm to fit BSLMM, which models both infinitesimal effects of all SNPs and large effects of a small subset of SNPs, to substantially reduce replication failure rate in real data.
50. Zhang, W., Najafabadi, H. & Li, Y. SparsePro: an efficient fine-mapping method integrating summary statistics and functional annotations. *PLoS Genet.* **19**, e1011104 (2023).
51. Lu, Z. et al. Improved multi-ancestry fine-mapping identifies *cis*-regulatory variants underlying molecular traits and disease risk. Preprint at *medRxiv* https://doi.org/10.1101/2024.04.15.24305836 (2024).
52. Rossen, J. et al. MultiSuSiE improves multi-ancestry fine-mapping in all of us whole-genome sequencing data. Preprint at *medRxiv* https://doi.org/10.1101/2024.05.13.24307291 (2024).
53. Zhang, X., Jiang, W. & Zhao, H. Integration of expression QTLs with fine mapping via SuSiE. *PLoS Genet.* **20**, e1010929 (2024).
54. Zhao, S. et al. Adjusting for genetic confounders in transcriptome-wide association studies improves discovery of risk genes of complex traits. *Nat. Genet.* **56**, 336–347 (2024).
This paper proposes a TWAS fine-mapping method that adapts SuSiE to fine-map genetically regulated expression of genes while controlling for horizontal pleiotropic effects of SNPs.
55. Strober, B. J., Zhang, M. J., Amariuta, T., Rossen, J. & Price, A. L. Fine-mapping causal tissues and genes at disease-associated loci. *Nat. Genet.* **57**, 42–52 (2025).
56. Akdeniz, B. C. et al. Finemap-MiXeR: a variational Bayesian approach for genetic finemapping. *PLoS Genet.* **20**, e1011372 (2024).
57. Cai, M. et al. XMAP: cross-population fine-mapping by leveraging genetic diversity and accounting for confounding bias. *Nat. Commun.* **14**, 6870 (2023).
58. Blei, D. M., Kucukelbir, A. & McAuliffe, J. D. Variational inference: a review for statisticians. *J. Am. Stat. Assoc.* **112**, 859–877 (2017).
59. Carbonetto, P. & Stephens, M. Scalable variational inference for Bayesian variable selection in regression, and its accuracy in genetic association studies. *Bayesian Anal.* **7**, 73–107 (2012).
60. Servin, B. & Stephens, M. Imputation-based analysis of association studies: candidate regions and quantitative traits. *PLoS Genet.* **3**, e114 (2007).
61. Ma, Y. & Zhou, X. Genetic prediction of complex traits with polygenic scores: a statistical review. *Trends Genet.* **37**, 995–1011 (2021).
62. Zhou, X., Carbonetto, P. & Stephens, M. Polygenic modeling with Bayesian sparse linear mixed models. *PLoS Genet.* **9**, e1003264 (2013).
This paper proposes BSLMM, a model that bridges the gap between sparse and infinitesimal genetic architectures to enable fine-mapping in the presence of a polygenic background, laying the groundwork for later methods such as SuSiE-inf and XMAP.
63. Zheng, Z. et al. Leveraging functional genomic annotations and genome coverage to improve polygenic prediction of complex traits within and between ancestries. *Nat. Genet.* **56**, 767–777 (2024).
64. Wu, Y. et al. Genome-wide fine-mapping improves identification of causal variants. Preprint at *medRxiv* https://doi.org/10.1101/2024.07.18.24310667 (2024).
65. Gjoka, A. & Cordell, H. J. Fine-mapping the results from genome-wide association studies of primary biliary cholangitis using SuSiE and h2-D2. *Genet. Epidemiol.* **49**, e22592 (2025).
66. The 1000 Genomes Project Consortium. A global reference for human genetic variation. *Nature* **526**, 68–74 (2015).
67. The ENCODE Project Consortium. An integrated encyclopedia of DNA elements in the human genome. *Nature* **489**, 57–74 (2012).
68. Roadmap Epigenomics Consortium et al. Integrative analysis of 111 reference human epigenomes. *Nature* **518**, 317–330 (2015).
69. Kircher, M. et al. A general framework for estimating the relative pathogenicity of human genetic variants. *Nat. Genet.* **46**, 310–315 (2014).
70. McLaren, W. et al. The Ensembl Variant Effect Predictor. *Genome Biol.* **17**, 122 (2016).
71. Wang, K., Li, M. & Hakonarson, H. ANNOVAR: functional annotation of genetic variants from high-throughput sequencing data. *Nucleic Acids Res.* **38**, e164 (2010).
72. Gazal, S. et al. Functional architecture of low-frequency variants highlights strength of negative selection across coding and non-coding annotations. *Nat. Genet.* **50**, 1600–1607 (2018).
73. Gazal, S. et al. Linkage disequilibrium-dependent architecture of human complex traits shows action of negative selection. *Nat. Genet.* **49**, 1421–1427 (2017).
74. Pickrell, J. K. Joint analysis of functional genomic data and genome-wide association studies of 18 human traits. *Am. J. Hum. Genet.* **94**, 559–573 (2014).
75. Alenazi, A. A., Cox, A., Juarez, M., Lin, W. Y. & Walters, K. Bayesian variable selection using partially observed categorical prior information in fine-mapping association studies. *Genet. Epidemiol.* **43**, 690–703 (2019).
76. Jiang, J. et al. Functional annotation and Bayesian fine-mapping reveals candidate genes for important agronomic traits in Holstein bulls. *Commun. Biol.* **2**, 212 (2019).
77. Wang, Q. S. et al. Leveraging supervised learning for functionally informed fine-mapping of cis-eQTLs identifies an additional 20,913 putative causal eQTLs. *Nat. Commun.* **12**, 3394 (2021).

78. Yang, J., Fritsche, L. G., Zhou, X., Abecasis, G. & International Age-Related Macular Degeneration Genomics Consortium. A scalable Bayesian method for integrating functional information in genome-wide association studies. *Am. J. Hum. Genet.* **101**, 404–416 (2017).
79. Do, C. B. & Batzoglou, S. What is the expectation maximization algorithm? *Nat. Biotechnol.* **26**, 897–899 (2008).
80. Kim, A. et al. Inferring causal cell types of human diseases and risk variants from candidate regulatory elements. Preprint at *medRxiv* https://doi.org/10.1101/2024.05.17.24307556 (2024).
81. Finucane, H. K. et al. Partitioning heritability by functional annotation using genome-wide association summary statistics. *Nat. Genet.* **47**, 1228–1235 (2015).
82. Albert, F. W. & Kruglyak, L. The role of regulatory variation in complex traits and disease. *Nat. Rev. Genet.* **16**, 197–212 (2015).
83. Bush, W. S., Oetjens, M. T. & Crawford, D. C. Unravelling the human genome-phenome relationship using phenome-wide association studies. *Nat. Rev. Genet.* **17**, 129–145 (2016).
84. van Rheenen, W., Peyrot, W. J., Schork, A. J., Lee, S. H. & Wray, N. R. Genetic correlations of polygenic disease traits: from theory to practice. *Nat. Rev. Genet.* **20**, 567–581 (2019).
85. Asimit, J. L. et al. Stochastic search and joint fine-mapping increases accuracy and identifies previously unreported associations in immune-mediated diseases. *Nat. Commun.* **10**, 3216 (2019).
86. Hernandez, N. et al. The flashfm approach for fine-mapping multiple quantitative traits. *Nat. Commun.* **12**, 6147 (2021).
87. Arvanitis, M., Tayeb, K., Strober, B. J. & Battle, A. Redefining tissue specificity of genetic regulation of gene expression in the presence of allelic heterogeneity. *Am. J. Hum. Genet.* **109**, 223–239 (2022).
88. Xu, C., Ganesh, S. K. & Zhou, X. mtPGS: leverage multiple correlated traits for accurate polygenic score construction. *Am. J. Hum. Genet.* **110**, 1673–1689 (2023).
89. Giambartolomei, C. et al. Bayesian test for colocalisation between pairs of genetic association studies using summary statistics. *PLoS Genet.* **10**, e1004383 (2014).
90. Hormozdiari, F. et al. Colocalization of GWAS and eQTL signals detects target genes. *Am. J. Hum. Genet.* **99**, 1245–1260 (2016).
91. Wallace, C. A more accurate method for colocalisation analysis allowing for multiple causal variants. *PLoS Genet.* **17**, e1009440 (2021).
92. Bick, A. G. et al. Genomic data in the all of us research program. *Nature* **627**, 340–346 (2024).
93. Nagai, A. et al. Overview of the BioBank Japan Project: study design and profile. *J. Epidemiol.* **27**, S2–S8 (2017).
94. Bycroft, C. et al. The UK Biobank resource with deep phenotyping and genomic data. *Nature* **562**, 203–209 (2018).
95. Zaitlen, N., Pasaniuc, B., Gur, T., Ziv, E. & Halperin, E. Leveraging genetic variability across populations for the identification of causal variants. *Am. J. Hum. Genet.* **86**, 23–33 (2010).
96. Shi, H. et al. Localizing components of shared transethnic genetic architecture of complex traits from GWAS summary data. *Am. J. Hum. Genet.* **106**, 805–817 (2020).
97. Kichaev, G. & Pasaniuc, B. Leveraging functional-annotation data in trans-ethnic fine-mapping studies. *Am. J. Hum. Genet.* **97**, 260–271 (2015).
98. Wen, X., Luca, F. & Pique-Regi, R. Cross-population joint analysis of eQTLs: fine mapping and functional annotation. *PLoS Genet.* **11**, e1005176 (2015).
99. Zhou, F. et al. Leveraging information between multiple population groups and traits improves fine-mapping resolution. *Nat. Commun.* **14**, 7279 (2023).
100. The GTEx Consortium. The GTEx Consortium atlas of genetic regulatory effects across human tissues. *Science* **369**, 1318–1330 (2020).
101. Sun, B. B. et al. Genomic atlas of the human plasma proteome. *Nature* **558**, 73–79 (2018).
102. McVicker, G. et al. Identification of genetic variants that affect histone modifications in human cells. *Science* **342**, 747–749 (2013).
103. Shi, H. et al. Population-specific causal disease effect sizes in functionally important regions impacted by selection. *Nat. Commun.* **12**, 1098 (2021).
104. Gamazon, E. R. et al. A gene-based association method for mapping traits using reference transcriptome data. *Nat. Genet.* **47**, 1091–1098 (2015).
105. Gusev, A. et al. Integrative approaches for large-scale transcriptome-wide association studies. *Nat. Genet.* **48**, 245–252 (2016).
106. Li, Z., Gao, B. & Zhou, X. An alternative framework for transcriptome-wide association studies to detect and decipher gene-trait associations. Preprint at *bioRxiv* https://doi.org/10.1101/2025.03.14.643391 (2025).
107. Wainberg, M. et al. Opportunities and challenges for transcriptome-wide association studies. *Nat. Genet.* **51**, 592–599 (2019).
108. Mancuso, N. et al. Probabilistic fine-mapping of transcriptome-wide association studies. *Nat. Genet.* **51**, 675–682 (2019).
109. Lu, Z. et al. Multi-ancestry fine-mapping improves precision to identify causal genes in transcriptome-wide association studies. *Am. J. Hum. Genet.* **109**, 1388–1404 (2022).
110. Hill, W. G., Goddard, M. E. & Visscher, P. M. Data and theory point to mainly additive genetic variance for complex traits. *PLoS Genet.* **4**, e1000008 (2008).
111. Hivert, V. et al. Estimation of non-additive genetic variance in human complex traits from a large sample of unrelated individuals. *Am. J. Hum. Genet.* **108**, 962 (2021).
112. Lenz, T. L. et al. Widespread non-additive and interaction effects within HLA loci modulate the risk of autoimmune diseases. *Nat. Genet.* **47**, 1085–1090 (2015).
113. Goyette, P. et al. High-density mapping of the MHC identifies a shared role for HLA-DRB1*01:03 in inflammatory bowel diseases and heterozygous advantage in ulcerative colitis. *Nat. Genet.* **47**, 172–179 (2015).
114. Conomos, M. P., Miller, M. B. & Thornton, T. A. Robust inference of population structure for ancestry prediction and correction of stratification in the presence of relatedness. *Genet. Epidemiol.* **39**, 276–293 (2015).
115. Zhou, X. & Stephens, M. Genome-wide efficient mixed-model analysis for association studies. *Nat. Genet.* **44**, 821–824 (2012).
116. Yang, Z. et al. Fine-mapping in admixed populations using CARMA-X, with applications to Latin American studies. *Am. J. Hum. Genet.* **112**, 1215–1232 (2025).
117. Benner, C. et al. Prospects of fine-mapping trait-associated genomic regions by using summary statistics from genome-wide association studies. *Am. J. Hum. Genet.* **101**, 539–551 (2017).
118. Zhang, W., Lu, T., Sladek, R., Dupuis, J. & Lettre, G. Robust fine-mapping in the presence of linkage disequilibrium mismatch. Preprint at *bioRxiv* https://doi.org/10.1101/2024.10.29.620968 (2024).
119. Marouli, E. et al. Rare and low-frequency coding variants alter human adult height. *Nature* **542**, 186–190 (2017).
120. Hawkes, G. et al. Whole-genome sequencing analysis identifies rare, large-effect noncoding variants and regulatory regions associated with circulating protein levels. *Nat. Genet.* **57**, 626–634 (2025).
121. Tennessen, J. A. et al. Evolution and functional impact of rare coding variation from deep sequencing of human exomes. *Science* **337**, 64–69 (2012).
122. Barton, A. R., Sherman, M. A., Mukamel, R. E. & Loh, P. R. Whole-exome imputation within UK Biobank powers rare coding variant association and fine-mapping analyses. *Nat. Genet.* **53**, 1260–1269 (2021).
123. Li, B. & Leal, S. M. Methods for detecting associations with rare variants for common diseases: application to analysis of sequence data. *Am. J. Hum. Genet.* **83**, 311–321 (2008).
124. Wu, M. C. et al. Rare-variant association testing for sequencing data with the sequence kernel association test. *Am. J. Hum. Genet.* **89**, 82–93 (2011).
125. Sanderson, E. et al. Mendelian randomization. *Nat. Rev. Methods Primers* **2**, 6 (2022).
126. Yuan, Z. et al. Likelihood-based Mendelian randomization analysis with automated instrument selection and horizontal pleiotropic modeling. *Sci. Adv.* **8**, eabl5744 (2022).
127. Hou, K. et al. Causal effects on complex traits are similar for common variants across segments of different continental ancestries within admixed individuals. *Nat. Genet.* **55**, 549–558 (2023).
128. Ding, Y. et al. Polygenic scoring accuracy varies across the genetic ancestry continuum. *Nature* **618**, 774–781 (2023).
129. Hou, K. et al. Calibrated prediction intervals for polygenic scores across diverse contexts. *Nat. Genet.* **56**, 1386–1396 (2024).
130. Herrera-Luis, E., Benke, K., Volk, H., Ladd-Acosta, C. & Wojcik, G. L. Gene–environment interactions in human health. *Nat. Rev. Genet.* **25**, 768–784 (2024).
131. Benegas, G., Ye, C., Albors, C., Li, J. C. & Song, Y. S. Genomic language models: opportunities and challenges. *Trends Genet.* **41**, 286–302 (2025).
132. Klein, J. C. et al. A systematic evaluation of the design and context dependencies of massively parallel reporter assays. *Nat. Methods* **17**, 1083–1091 (2020).
133. Porto, E. M., Komor, A. C., Slaymaker, I. M. & Yeo, G. W. Base editing: advances and therapeutic opportunities. *Nat. Rev. Drug Discov.* **19**, 839–859 (2020).
134. Finucane, H. K. et al. Heritability enrichment of specifically expressed genes identifies disease-relevant tissues and cell types. *Nat. Genet.* **50**, 621–629 (2018).
135. Zhou, X. A unified framework for variance component estimation with summary statistics in genome-wide association studies. *Ann. Appl. Stat.* **11**, 2027–2051 (2017).
136. Kanai, M. et al. Insights from complex trait fine-mapping across diverse populations. Preprint at *medRxiv* https://doi.org/10.1101/2021.09.03.21262975 (2021).
137. Morris, J. A. et al. Discovery of target genes and pathways at GWAS loci by pooled single-cell CRISPR screens. *Science* **380**, eadh7699 (2023).
138. Lee, S. et al. Massively parallel reporter assay investigates shared genetic variants of eight psychiatric disorders. *Cell* **188**, 1409–1424.e21 (2025).

Acknowledgements
This study was supported by the National Institutes of Health (NIH) Grants R01HG009124 and R01GM144960. The funders had no role in study design, data collection and analysis, decision to publish, or preparation of the manuscript. The authors thank B. Gao for his help with interpreting the literature.

Author contributions
The authors contributed equally to all aspects of the article.

Competing interests
The authors declare no competing interests.

Additional information
Peer review information *Nature Reviews Genetics* thanks Jian Zeng, Bogdan Pasaniuc and the other, anonymous, reviewer(s) for their contribution to the peer review of this work.